

This article was downloaded by:

On: 14 January 2011

Access details: *Access Details: Free Access*

Publisher *Taylor & Francis*

Informa Ltd Registered in England and Wales Registered Number: 1072954 Registered office: Mortimer House, 37-41 Mortimer Street, London W1T 3JH, UK



## Molecular Simulation

Publication details, including instructions for authors and subscription information:

<http://www.informaworld.com/smpp/title~content=t713644482>

### Simulation of heat conduction in nanocomposite using energy-conserving dissipative particle dynamics

R. Qiao<sup>a</sup>; P. He<sup>a</sup>

<sup>a</sup> Department of Mechanical Engineering, Clemson University, Clemson, SC, USA

**To cite this Article** Qiao, R. and He, P.(2007) 'Simulation of heat conduction in nanocomposite using energy-conserving dissipative particle dynamics', *Molecular Simulation*, 33: 8, 677 — 683

**To link to this Article:** DOI: 10.1080/08927020701286511

**URL:** <http://dx.doi.org/10.1080/08927020701286511>

PLEASE SCROLL DOWN FOR ARTICLE

Full terms and conditions of use: <http://www.informaworld.com/terms-and-conditions-of-access.pdf>

This article may be used for research, teaching and private study purposes. Any substantial or systematic reproduction, re-distribution, re-selling, loan or sub-licensing, systematic supply or distribution in any form to anyone is expressly forbidden.

The publisher does not give any warranty express or implied or make any representation that the contents will be complete or accurate or up to date. The accuracy of any instructions, formulae and drug doses should be independently verified with primary sources. The publisher shall not be liable for any loss, actions, claims, proceedings, demand or costs or damages whatsoever or howsoever caused arising directly or indirectly in connection with or arising out of the use of this material.

# Simulation of heat conduction in nanocomposite using energy-conserving dissipative particle dynamics

R. QIAO\* and P. HE

Department of Mechanical Engineering, Clemson University, Clemson, SC 29634, USA

(Received January 2007; in final form February 2007)

We report on the simulation of heat conduction in nanocomposite by using a novel mesoscopic particle method, the energy-conserving dissipative particle dynamics (eDPD) method. The original eDPD method is extended to account for the interfacial thermal resistance occurs at the angstrom-wide interface between materials, and we also investigated the choice of time step in eDPD simulations. For nanocomposite with randomly dispersed nanoparticles, the eDPD simulations predict that the thermal conductivity of matrix material can be enhanced by embedding high thermal conductivity nanoparticles, but the effectiveness of such a strategy diminishes as the interfacial thermal resistance between the nanoparticle and matrix material increases. These results are in quantitative agreement with the classical Maxwell–Garnett model. Further simulations indicate that the enhancement of thermal conductivity can be affected by the alignment of nanoparticles with respect to the temperature gradient, which cannot be predicted by the classical models. These simulation results indicate that eDPD method can be a versatile method for studying thermal transport in heterogeneous materials and complex systems.

**Keywords:** Nanocomposite; Heat conduction; Interfacial thermal resistance; Energy-conserving dissipative particle dynamics; DPD; Mesoscale simulation

## 1. Introduction

Thermal transport plays a critical role in a wide array of engineering fields ranging from manufacturing, high power density microelectronics, to thermal processing [1]. A commonly encountered issue is the low thermal conductivity of the heat transfer medium (e.g. heat transfer fluid or polymeric matrix), which often renders the heat transfer inefficient. One possible solution to such a problem is to disperse high thermal conductivity particles (or wires and disks) into the original heat transfer medium to enhance its thermal conductivity. For solid composites, aluminum nitride particles (or whiskers) have been used as fillers to enhance the thermal conductivity of epoxy and polyimide matrix [2,3]. More recently, less abrasive solid particles (e.g. boron nitride), have been reported to enhance the thermal conductivity of polymeric matrix significantly [4]. Parallel with the development in solid composites, liquid dispersed with solid nanoparticles (termed “nanofluids”) has been shown to exhibit much higher thermal conductivity compared to the base fluids even for very low particle loading [5,6]. Most recently, it

was discovered that organic liquid with nanosized water droplet dispersed in it (termed “nanoemulsion”) also shows great thermal conductivity enhancement compared to the original fluid [7].

The effective thermal conductivity of these nanocomposites is affected by many physical processes, e.g. heat conduction inside the nanoparticle and host media. When the host media is fluid, microscale convection induced by the Brownian motion of nanoparticles has also been proposed to play an important role [8]. Recent studies also indicate that the interfacial thermal resistance between the embedding particle and host media plays a critical role in determining the effective thermal conductivity of the nanocomposite [9]. While the exact origins of the interfacial thermal resistance are not well understood at present, recent experiments indicate that such interfacial resistance are particularly significant between hydrophobic surface and polar fluids [10]. While the mechanism of thermal conductivity enhancement in solid composites seems to be well-understood and the classical effective medium theories, e.g. the Maxwell–Garnett theory [11], explain the experimental observation

\*Corresponding author. Email: rqiao@ces.clemson.edu; URL: <http://www.clemson.edu~rqiao>

well [12], the mechanisms of thermal conductivity enhancement in nanofluids and nanoemulsion are less well-understood and significant controversies exist. In particular, the role of nanoparticle Brownian motion in determining the heat conduction remains elusive [6], although empirical models suggest that the Brownian motion of nanoparticle may contribute significantly to the observed enhancements [8,13].

The effective thermal conductivity of nanocomposites depends on many design parameters, e.g. particle volume fraction and size (and shape) of nanoparticles. Understanding how these design parameters affect the interactions between the different physical processes mentioned above and thus the effective thermal conductivity of nanocomposite is crucial for the optimal design of these nanocomposites. While simulations based on solving thermal transport equations using finite difference or finite element methods can be useful, exploring a large parameter space can be cumbersome as generating high quality mesh for such heterogeneous materials is rather challenging. Effective medium theories, e.g. the Maxwell–Garnett theory, can be very effective in predicting the thermal conductivity for simple particle geometries [11]. However, the correlation of heat conduction near neighboring nanoparticles is not accounted for and the particles are assumed to be randomly dispersed in the host matrix. In addition, these theoretical approaches can be difficult to apply when the shape of particle is complicated and when the particles are polydispersed. Particle simulation can be very appealing in such a situation. However, classical MD simulation is often difficult to use due to the high computational cost. In fact, unless the embedding particle is smaller than a few nanometers, it is often not necessary to model the thermal and transport process with atomistic resolution. In such a scenario, coarse-grained methods, in which fluid and nanoparticles are resolved at a length scale comparable to the scale of nanoparticle (or their spacing), can be very useful.

In this paper, we study the heat conduction in nanocomposite by using a mesoscopic particle method, namely the energy-conserving dissipative particle dynamics (eDPD) method. We show that by extending the standard eDPD model, it is possible to incorporate atomistic effects into the mesoscopic simulations and to predict the heat conduction in nanocomposite with good accuracy. The rest of the paper is organized as follows. Section 2 presents the eDPD method, Section 3 discusses the validation of the eDPD code and its application to simulation of heat conduction in nanocomposite. Finally, conclusions are presented in Section 4.

## 2. Energy-conserving dissipative particle dynamics

### 2.1 Basic formulations

Dissipative particle dynamics (DPD) is a mesoscopic method developed for modeling complex fluids [14,15].

The original model is limited to isothermal applications. A more general model, namely the eDPD model, was developed to extend its applicability to thermal simulations [16,17]. Particles in an eDPD model are coarse-grained entities representing a patch of molecules. These particles are characterized by their mass, position, velocity, heat capacity and temperature (internal energy). For simplicity of presentation, we assume that all particles have the same mass and heat capacity. eDPD particles interact with each other via three types of forces: a repulsive conservative force, a dissipative force that reduces the velocity difference between particles, and a random force acting along the line connecting the particles. In addition, eDPD particles exchange energy via a “collisional” heat flux and a random heat flux. An eDPD system evolves via [16]:

$$d\mathbf{r}_i = \mathbf{v}_i dt \quad (1)$$

$$m d\mathbf{v}_i = \mathbf{F}_i^C dt + \mathbf{F}_i^D dt + \mathbf{F}_i^R \sqrt{dt} \quad (2)$$

$$C_v dT_i = q_i^{\text{visc}} dt + q_i^{\text{cond}} dt + q_i^{\text{rand}} \sqrt{dt} \quad (3)$$

where  $m$ ,  $C_v$ ,  $\mathbf{r}_i$ ,  $\mathbf{v}_i$ ,  $T_i$  are the mass, heat capacity, position, velocity and temperature of particle  $i$ , respectively.  $\mathbf{F}_i^C$ ,  $\mathbf{F}_i^D$  and  $\mathbf{F}_i^R$  are the conservative, dissipative and random forces acting on particle  $i$ , respectively.  $q_i^{\text{visc}}$  accounts for the viscous heating due to the dissipative interactions between the particles.  $q_i^{\text{cond}}$  and  $q_i^{\text{rand}}$  are the collisional and random heat fluxes acting on particle  $i$ . These forces and heat fluxes are given by Ref. [16]:

$$\mathbf{F}_i^C = \sum_{j \neq i} a_{ij} w(r_{ij}/r_c) \mathbf{e}_{ij} \quad (4)$$

$$\mathbf{F}_i^D = \sum_{j \neq i} -\gamma_{ij} w^2(r_{ij}/r_c) (\mathbf{e}_{ij} \cdot \mathbf{v}_{ij}) \mathbf{e}_{ij} \quad (5)$$

$$\mathbf{F}_i^R = \sigma_{ij} w(r_{ij}/r_c) \theta_{ij} \mathbf{e}_{ij} \quad (6)$$

$$q_i^{\text{cond}} = \sum_{j \neq i} \kappa_{ij} w^2(r_{ij}/r_s) \left( \frac{1}{T_i} - \frac{1}{T_j} \right) \quad (7)$$

$$q_i^{\text{rand}} = \sum_{j \neq i} \alpha_{ij} w(r_{ij}/r_s) \theta_{ij}^e \quad (8)$$

$$q_i^{\text{visc}} = \frac{1}{2C_v} \sum_{j \neq i} \left( w^2(r_{ij}/r_c) \left[ \gamma_{ij} (\mathbf{e}_{ij} \cdot \mathbf{v}_{ij})^2 - \frac{1}{m} \sigma_{ij}^2 \right] - \sigma_{ij} w(r_{ij}/r_c) (\mathbf{e}_{ij} \cdot \mathbf{v}_{ij}) W_{ij} \right) \quad (9)$$

where  $a_{ij}$  is the conservative force coefficient and  $r_{ij} = |\mathbf{r}_{ij}| = |\mathbf{r}_i - \mathbf{r}_j|$ .  $r_c$  and  $r_s$  are the cutoff lengths for momentum and energy exchanges.  $w$  is a weighting function. Two types of weighting functions are widely used, namely, the linear weighting function and the Lucy weighting function [18]. The linear weighting function

takes the form

$$w(r) = \begin{cases} 1 - r & \text{if } r < 1.0 \\ 0 & \text{otherwise} \end{cases} \quad (10)$$

and Lucy weighting function is

$$w(r) = \begin{cases} \frac{105}{16\pi}(1 + 3r)(1 - r)^3 & \text{if } r < 1.0 \\ 0 & \text{otherwise} \end{cases} \quad (11)$$

In the present paper, the linear weighting function is used.  $\mathbf{e}_{ij} = \mathbf{r}_{ij}/r_{ij}$ , and  $\mathbf{v}_{ij} = \mathbf{v}_i - \mathbf{v}_j$ .  $\theta_{ij}$  and  $\theta_{ij}^c$  are symmetric and anti-symmetric random variables with zero mean and unit variance, respectively. Though the original DPD method uses Gaussian random variables, recent studies indicate that using uniform random variables produces essentially the same results [19,20]. Since the generation of uniform random numbers are computationally less expensive,  $\theta_{ij}$  and  $\theta_{ij}^c$  are generated by using a uniform random number generator in the present paper. Variables  $\gamma_{ij}$  and  $\sigma_{ij}$  determine the strength of the dissipative and random force, and variables  $\kappa_{ij}$  and  $\alpha_{ij}$  determine the strength of the collisional and random heat flux. The Fluctuation–Dissipation theorem requires that

$$\gamma_{ij} = \sigma_{ij}^2(T_i + T_j)/4k_B T_i T_j \quad (12)$$

$$\kappa_{ij} = \alpha_{ij}^2/2k_B \quad (13)$$

where  $k_B$  is the Boltzmann constant. Usually  $\sigma_{ij}$  is taken as a constant and

$$\kappa_{ij} = C_v \bar{\kappa}(T_i + T_j)^2/4\lambda^2 \quad (14)$$

where  $\lambda$  is the mean particle spacing.  $\bar{\kappa}$  has a unit of  $\text{m}^2/\text{s}$ , and can be interpreted as a particle thermal diffusivity.  $\bar{\kappa}$  is often expressed as

$$\bar{\kappa} = \lambda^2 \kappa_0 C_v/k_B \quad (15)$$

where  $\kappa_0$  is a constant controlling the thermal conductivity of eDPD beads. The heat capacity of an eDPD bead is usually measured by the dimensionless heat capacity  $\bar{C}_v = C_v/k_B$ . With the above choices, the collisional heat flux between two particles is proportional to their temperature difference and shows least dependence on the absolute temperature [18]. Variables in DPD models are presented in reduced units, and mass, length and energy are measured by  $m$ ,  $r_c$ ,  $k_B T$ , respectively.

Though the original DPD model is heuristic in nature, theoretical foundations of the DPD model have been established recently. An  $\mathcal{H}$ -theorem, which ensures that there exists a unique equilibrium state, was proved in Ref. [18]. DPD model has been shown to produce correct hydrodynamic behavior, i.e. the Navier–Stokes equations emerges at long wave length limit and a unique viscosity can be defined [21]. These theoretical works are well supported by the numerical simulations [22,23]. While the isothermal DPD method has received significant attention in the past years, the energy-conserving DPD method received scant attention [22,24–26]. In this paper, we

investigate the heat conduction in nanocomposite using the eDPD method.

## 2.2 Introducing interfacial thermal resistance into eDPD model

As discussed in Section 1, interfacial thermal resistance between embedding particle and host matrix material plays an important role in determining the effective thermal conductivity of a nanocomposite. However, modeling interfacial thermal resistance directly in eDPD simulation essentially means that the level of coarse-graining is comparable to atomistic scale, and this will render the simulation inefficient. Here, we propose to incorporate the effects of interfacial thermal resistance by modifying the  $\kappa_{ij}$  term of the “collisional” heat flux  $q_{\text{cond}}$  shown in equation (7). Specifically, we now define

$$\kappa_{ij} = C_v \bar{\kappa}(T_i + T_j)^2/4(\lambda^2 + \Lambda R_b \lambda) \quad (16)$$

where  $\Lambda$  is the bulk thermal conductivity of the solid, and  $R_b$  is the interfacial resistance between embedding particles and the matrix material. The essential idea behind equation (16) is that the interfacial thermal resistance effectively increases the distance between the two thermally-interacting particles. The increased distance,  $\Lambda R_b$ , is the so-called “Kapitza length” [5], and is equal to the thickness of matrix material that has the same thermal resistance as the interfacial thermal resistance.

## 3. Results and discussion

A simulation code based on the eDPD models described by equations (1)–(16) has been developed. The equation of motion is integrated by using the method described in Refs. [19,20]. Since we are primarily interested in the heat conduction in solid nanocomposite, velocities of all particles (both matrix beads and nanoparticle beads) are set to zero. In such a case, the conservative, dissipative and random forces in equations (4)–(6) are all zero.

### 3.1 Code validation

We first study the thermal equilibrium in a random eDPD solid. The simulation system consists of 4096 particles randomly distributed in a periodic box of  $10.08 \times 10.08 \times 10.08$ . Initially, the temperature of all eDPD beads was set to 1.0. Two dimensionless heat capacities  $\bar{C}_v$ , 60.0 and 120.0 were used in the simulations. Time step size ( $\Delta t$ ) was varied from 0.005 to 0.04 in different runs. An equilibrium run of 50,000 step was first performed, and was followed by a production run of at least 100,000 steps.

Figure 1 shows a representative snapshot of the simulation system ( $\bar{C}_v = 120.0$ ) at thermal equilibrium. The color of eDPD beads are coded by the their instantaneous temperature. We observe that the temperature



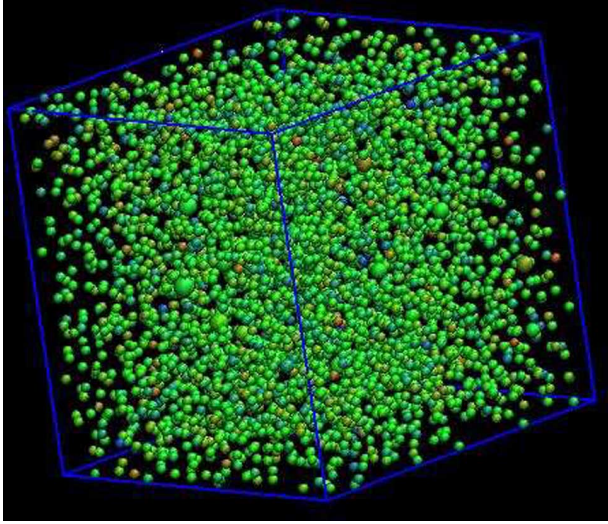


Figure 1. Temperature distribution inside a random eDPD solid. The average temperature is 1.0 (colored as green in the figure). The dimensionless heat capacity of the eDPD particles is 120.0. Figure was rendered by using VMD [28].

(or equivalently the internal energy  $\epsilon$ ) of eDPD particles is not uniform at thermal equilibrium. To quantify the distribution of particle's internal energy, we compute the one-particle energy distribution function  $\psi(\epsilon)$ . It has been shown that for eDPD particles with large heat capacity,  $\psi(\epsilon)$  is given by Refs. [24,22]:

$$\psi(\epsilon) = \frac{\beta}{\Gamma(\bar{C}_v + 1)} (\beta\epsilon)^{\bar{C}_v} \exp(-\beta\epsilon) \quad (17)$$

where  $\epsilon = C_v T$ ,  $\Gamma(x)$  is the gamma function and  $\beta = 1/k_B T$ . Figure 2 compares the eDPD simulation results with the prediction of equation (17). We observe that the relative scattering of internal energy with respect to its mean energy becomes smaller as  $\bar{C}_v$  increases and excellent agreement between the eDPD simulation and analytical predictions is obtained. The narrower distribution of the internal energy can be understood by noting that, as  $\bar{C}_v$

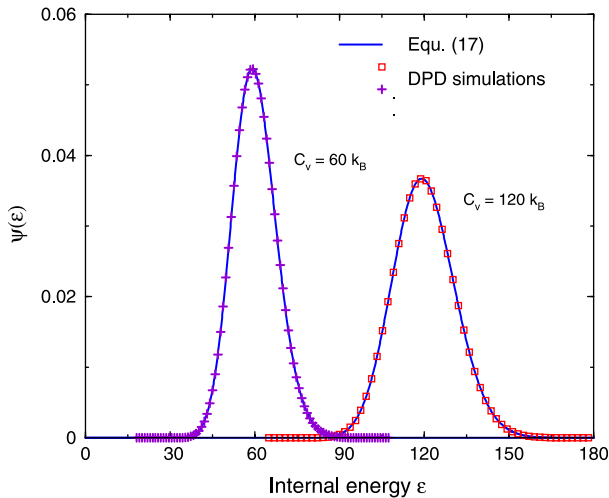


Figure 2. Equilibrium distribution of the internal energy of eDPD particles inside a random eDPD solid with heat capacities of 60 and 120. The time step size of eDPD simulation is 0.01.

increases, the eDPD particles become more coarse-grained, and thus exhibit less fluctuations in its internal energy [24].

The choice of time step in simulation of eDPD solid has not been investigated so far. While large time step is usually desired in particle simulations, too large a time step may cause substantial artifacts [27]. In the simulation of isothermal DPD fluids, time step size is often chosen to ensure that the fluid temperature does not deviate significantly from a pre-set value. Since the average temperature in an equilibrium eDPD simulation is always a constant (unless the time step is so large that some eDPD beads reach negative temperature and thus crushes the simulation), it is not clear how to determine the upper limit of the time step size. Specially, while a moderately large time step may allow the simulation to be performed, it is not clear whether such time step is small enough to reproduce the correct thermal behavior. One possible way of establishing a more conservative maximum time step size in equilibrium simulations is to monitor how well the eDPD simulation reproduces the one-particle energy distribution. Here, we tested five different  $\Delta t$  in the range of 0.005–0.04 by monitoring the average temperature and one-particle energy distribution. It is found that while simulation crushed within a few thousand steps for  $\Delta t > 0.035$ , the system temperature is maintained perfectly if  $\Delta t \leq 0.035$ . It is also found that for  $\Delta \leq 0.035$ , the deviation of the one-particle energy distribution function obtained in the eDPD simulation from that predicted by equation (17) is negligible. This seems to suggest that, for equilibrium simulations, it is reasonable to use large time step as long as the simulation does not produce negative temperature (and thus crushes). However, further tests are needed (e.g. studying the sensitivity of the thermal conductivity of eDPD solids to the time step size) before a firm conclusion can be made.

We next test the code by studying the heat conduction in a slab of eDPD solid (lateral dimension:  $20 \times 20$ ; height  $H$ : 66). The solid particles are evenly spaced with a lattice spacing of  $2/3$ . Each wall is made of two layers of eDPD solid particles with the same lattice spacing. The temperature of the lower and upper walls are fixed at 1.0 and 2.0, respectively. At  $t = 0$ , temperature of the slab particles is 1.5. The dimensionless heat capacity of the eDPD particle is set to  $\bar{C}_v = 1 \times 10^5$ , and  $\kappa_0 = 0.1$ . With such a large  $\bar{C}_v$ , the system essentially evolves deterministically, and thus facilitates the comparison of the eDPD simulation results with available analytical solution

$$\begin{aligned} T(x, t) = & \left( \frac{x}{H} + \frac{1}{2} \right) + \frac{2}{\pi} \sum_{i=1}^{\infty} \sin \left[ (2i-1) \pi \frac{x}{H} \right] \\ & \times \exp \left[ -(2i-1)^2 \pi^2 D / H^2 t \right] \\ & + \frac{2}{\pi} \sum_{i=1}^{\infty} \frac{(-1)^i}{i} \sin \left[ i \pi \left( \frac{x}{H} + \frac{1}{2} \right) \right] \\ & \times \exp \left[ -(i\pi)^2 D / H^2 t \right] \end{aligned} \quad (18)$$

where  $D$  is the thermal diffusivity of slab. Simulation was performed by using a time step of  $5 \times 10^{-5}$ . To investigate whether the eDPD simulation can predict the evolution of temperature field in the eDPD solid, we fitted the eDPD results to analytical solution equation (18) by using the thermal diffusivity as a fitting parameter. Figure 3(a) shows the eDPD solution and the fitted equation (18) with  $D = 1.72 \times 10^3$ . Alternatively, we calculated the heat diffusivity by first computing the thermal conductivity of slab and then dividing the thermal conductivity by heat capacity of the eDPD slab. The  $D$  obtained agrees perfectly with the  $D$  obtained from the above procedure. We thus conclude that eDPD simulation can reproduce the heat conduction process well. We also performed the simulation at higher temperatures, and the same thermal diffusivity was obtained. This indicates that the thermal diffusivity (and thus thermal conductivity) of an eDPD solid is insensitive to its temperature.

To test the interfacial thermal resistance model described in Section 2, the problem in figure 3(A) was re-done with an interfacial thermal resistance  $R_b = 19\lambda/\Lambda$  introduced between the wall and the eDPD solid ( $\lambda$  is the lattice spacing between particles). Figure 3(B) shows the steady-state temperature profile in the solid. In excellent agreement with the analytical solution, a temperature drop of 0.140 is observed at both walls.

### 3.2 Heat conduction in nanocomposite

Here, we study the heat conduction in a solid nanocomposite. The simulation system consists of a cubic box ( $12 \times 12 \times 12$ ) of nanocomposite enclosed by two walls. The nanocomposite is made of 0–4 nanoparticles (diameter  $D_p$ : 3.66) randomly dispersed in an eDPD solid matrix (number density  $n = 10.0$ ).  $\kappa_0$  of the eDPD particles belong to host matrix and nanoparticles

are set to 0.0001 and 0.002, respectively. The dimensionless heat capacity of the eDPD particles are 2000.0 for both the nanoparticle and solid matrix. To obtain the length scale of the eDPD simulation, we note that the total heat capacity of a unit volume in the eDPD simulation is  $n\bar{C}_v$ , which corresponds to the total heat capacity of real materials in a volume of  $[L]^3$ . Therefore,  $n\bar{C}_v k_B = [L]^3 \rho_{\text{real}} C_{v,\text{real}}$  where  $\rho_{\text{real}}$  and  $C_{v,\text{real}}$  are the density and heat capacity of real materials. It follows that  $[L] = (n\bar{C}_v k_B / \rho_{\text{real}} C_{v,\text{real}})^{1/3}$ . If we map the eDPD particles to Pyrex glass ( $\rho = 2.23 \times 10^3 \text{ kg/m}^3$ ,  $C_v = 753 \text{ J/(kgK)}$ ), then with the eDPD parameters chosen here,  $[L] = 5.48 \text{ nm}$ . This produces a dimensional diameter of 20 nm for the nanoparticles embedded in the host matrix.

To compute the thermal conductivity of the nanocomposite, we set the temperature of the left and right walls enclosing the nanocomposite to 1.0 and 2.0, respectively. We then perform long simulation (time  $> 2000$ ) so that the heat conduction in the nanocomposite reaches a steady-state. We then continue the simulation for a time of 1000.0 to obtain the heat flux  $Q$ . In solid eDPD systems, the heat flux is given by Ref. [24]

$$Q = \sum_{i=1}^N \sum_{j>i} \left[ \kappa_{ij} w^2(r_{ij}/r_s) \left( \frac{1}{T_i} - \frac{1}{T_j} \right) \right] \mathbf{r}_{ij} \quad (19)$$

The effective thermal conductivity of nanocomposite is computed by using the Fourier law  $\kappa_c = -Q\Delta L/\Delta T$ , where  $\Delta L = 12.0$  and  $\Delta T = 1.0$  in all the simulations.

We performed two series of simulations to investigate the heat conduction enhancement in nanocomposites. In the first series of simulations, the interfacial thermal resistance between nanoparticles and solid matrix materials is zero, while in the second series of simulation, an interfacial thermal resistance of  $12.6 D_p/k_m$  is introduced between the nanoparticles and solid matrix materials. The effective thermal conductivity of such a nanocomposite can be described by the classical Maxwell–Garnett (M–G) model [11]:

$$\frac{k_c}{k_m} = \frac{2 + \beta(1 + 2\alpha) + 2\phi[\beta(1 - \alpha) - 1]}{2 + \beta(1 + 2\alpha) - \phi[\beta(1 - \alpha) - 1]} \quad (20)$$

where  $k_c$  and  $k_m$  are the thermal conductivity of nanocomposite and host matrix, respectively.  $\phi$  is the particle volume fraction and  $\beta$  is the thermal conductivity ratio of nanoparticle and host matrix, and  $\alpha = 2R_b k_m/D_p$ .

Figure 4(A), (B) shows the instantaneous temperature distribution inside nanocomposite with four embedding nanoparticles ( $R_b = 0$ ). We observe that there exist noticeable fluctuations of temperature inside the simulation domain and that the temperature is relatively uniform inside the nanoparticles, which is consistent with the higher thermal conductivity of the nanoparticles. Figure 5 compares the thermal conductivity enhancement of nanocomposite as predicted by the M–G theory equation (20) and the eDPD simulations. These results indicate that while nanoparticle inclusion can enhance heat conduction of the matrix material when the interfacial

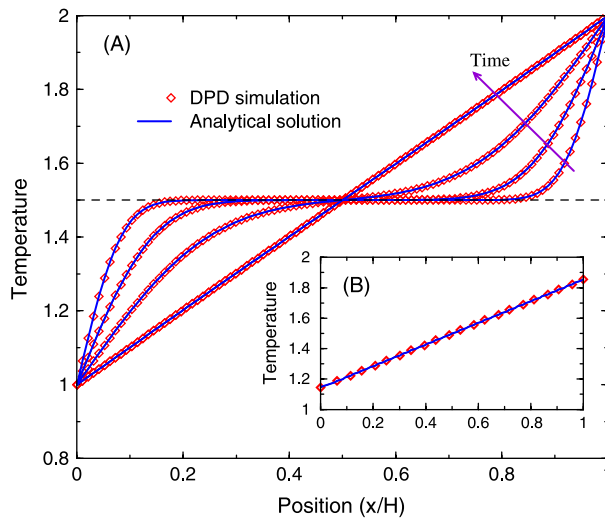


Figure 3. Heat conduction in a slab of eDPD solid enclosed by two walls: (A) temperature evolution in the solid at  $t = 0.005, 0.015, 0.045$  and  $0.3$ . The interfacial thermal resistance between wall and solid is zero; (B) steady-state temperature distribution in the solid when an interfacial heat resistance of  $19\lambda/\Lambda$  is introduced between the slab and wall particles.

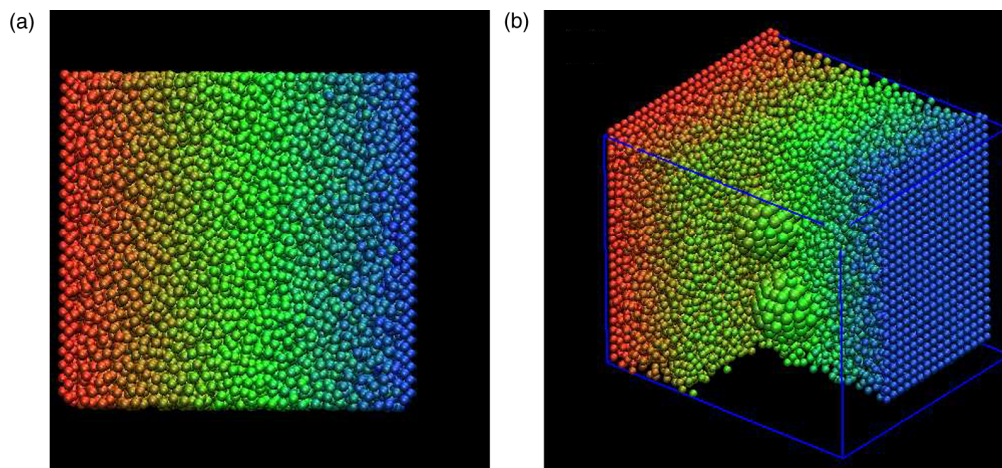


Figure 4. (A) Side view of temperature distribution in the solid nanocomposite. (B) Temperature distribution inside the solid nanocomposite. For clarity purpose, the beads in the region  $[x > 5.0; y > 7.0]$  (except the embedding particles) were removed. The blue line denotes the periodic boundary of the simulation box. Figures were rendered by using VMD [28].

thermal resistance between nanoparticle and solid matrix is negligible, it can actually decrease the heat conduction if the interfacial thermal resistance is significant. The good agreement between the M–G theory and eDPD simulation results shows the eDPD method can be used effectively for solving thermal transport problem in heterogeneous materials.

In the classical M–G model, nanoparticles are assumed to be randomly dispersed in the host matrix. Here, we further study the effective thermal conductivity of nanocomposite in which nanoparticles are aligned with respect to the temperature gradient. We consider two extreme cases. In the first case, three nanoparticles are aligned normal to the temperature gradient (figure 6), and in the second case, the three nanoparticles are aligned in the temperature gradient direction. Figure 6 compares the enhancement of effective thermal conductivity for the two cases with the classical M–G model. We observe that while the deviation from M–G prediction is small when

nanoparticles are aligned normal to the temperature gradient, the enhancement is substantially stronger when nanoparticles are aligned along the temperature gradient direction. The smaller effective thermal conductivity for vertical alignment case compared to the M–G prediction may be caused by the fact that nanoparticles in such a configuration provide a less efficient heat conduction pathway (in the temperature gradient direction) than the homogeneous nanoparticle configuration assumed in the M–G theory.

#### 4. Conclusions

In summary, we studied thermal equilibrium and heat conduction in single-component solids and nanocomposites using the eDPD method. The simulation results indicate that

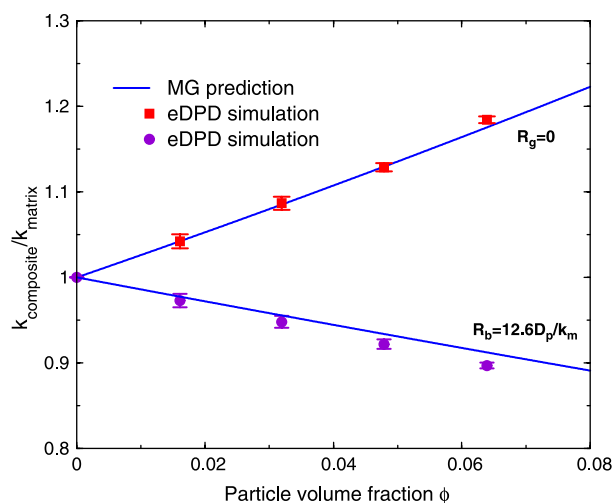


Figure 5. Comparison of thermal conductivity enhancement of solid nanocomposite as predicted by the M–G theory equation (20) and the eDPD simulations for different interfacial thermal resistance between nanoparticle and host solid matrix.

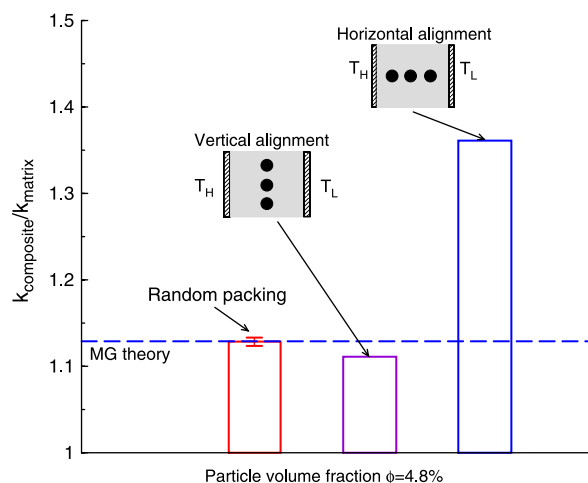


Figure 6. Comparison of thermal conductivity enhancement of solid nanocomposite as predicted by the M–G theory equation (20) and the eDPD simulations when the nanoparticles are aligned. The volume fraction of nanoparticles in the nanocomposite is 4.8%, and the interfacial thermal resistance is zero.



1. The effects of interfacial thermal resistance, an atomistic phenomenon, can be incorporated into the mesoscopic eDPD simulation by modifying the “collisional” heat flux in equation (7).
2. The eDPD method can be used to compute the effective thermal conductivity of heterogeneous nanocomposite effectively. Calculations indicate that the thermal conductivity of matrix materials can be enhanced by embedding high thermal conductivity nanoparticles. Such enhancement can be described well by the classical Maxwell–Garnett model when the nanoparticles are dispersed randomly. The eDPD simulations also indicate that the alignment of nanoparticles with respect to the temperature gradient can affect the thermal conductivity enhancement significantly, which cannot be predicted by the Maxwell–Garnett model.

Together, these results show that the mesoscopic eDPD method can be used to solve complicated heat conduction problems that involve physical processes at length scales ranging from angstrom level to continuum level. Combined with the intrinsic advantage of particle methods in modeling complex and heterogeneous geometry, the results obtained here shows that eDPD method is a promising multiscale method for solving complex thermal transport problems. In the present study, the motion of matrix material and nanoparticles is quenched to minimize the possible complications due to the Brownian motion of nanoparticles. To incorporate the thermal motion of nanoparticles in eDPD simulations, one need to explicitly compute the conservative, dissipative and random force in equations (4)–(6), and then integrate the equation of motion for all eDPD beads. Such simulations can be useful in elucidating the effects of Brownian motion on the overall thermal transport in nanofluids, and will be a subject of future investigation.

## Acknowledgements

The authors gratefully acknowledge the financial support from Clemson University.

## References

- [1] F.P. Incropera, D.P. DeWitt, T.L. Bergman, A.S. Lavine. *Fundamentals of Heat and Mass Transfer*, 6th ed., John Wiley and Sons, New York (2006).
- [2] L. Li. Thermally conducting polymer-matrix composites containing both carbon particles and carbon whiskers. *J. Electron. Mater.*, **23** (1994).
- [3] Y.S. Xu, D.D.L. Chung, C. Mroz. Thermally conducting aluminum nitride polymer-matrix composites. *Composites part A: Appl. Sci. Manufact.*, **32**, 1749 (2001).
- [4] H.Y. Ng, S.K. Lau, X.H. Lu. Thermal conductivity, thermo-mechanical and rheological studies of boron nitride-filled polybutylene terephthalate. *Mater. Sci. Forum.*, **437–438**, 239 (2003).
- [5] J.A. Eastman, S.R. Phillpot, S.U.S. Choi, P. Keblinski. Thermal transport in nanofluids. *Annu. Rev. Mater. Res.*, **34**, 219 (2004).
- [6] P. Keblinski, J.A. Eastman, D.G. Cahill. Nanofluids for thermal transport. *Mater. Today*, **8**, 36 (2005).
- [7] B. Yang, Z.H. Han. Thermal conductivity enhancement in water-in-oil nanoemulsion fluids. *Appl. Phys. Lett.*, **88**, 21914 (2006).
- [8] R.S. Prasher, P. Bhattacharya, P.E. Phelan. Thermal conductivity of nanoscale colloidal solutions (nanofluids). *Phys. Rev. Lett.*, **94**, 025901 (2005).
- [9] S.T. Huxtable, D.G. Cahill, S. Shenogin, L.P. Xue, R. Ozisik, P. Barone, M. Usrey, M.S. Strano, G. Siddon, M. Shim, P. Keblinski. Interfacial heat flow in carbon nanotube suspensions. *Nat. Mater.*, **2**, 731 (2003).
- [10] O.M. Wilson, X.Y. Hu, D.G. Cahill, P.V. Braun. Colloidal metal particles as probes of nanoscale thermal transport in fluids. *Phys. Rev. B*, **66**, 224301 (2002).
- [11] C.W. Nan, R. Birringer, D.R. Clarke, H. Gleiter. Effective thermal conductivity of particulate composites with interfacial thermal resistance. *J. Appl. Phys.*, **81**, 6692 (1997).
- [12] A. Boudenne, L. Ibos, M. Fois, E. Gehin, J.C. Majeste. Thermophysical properties of polypropylene/aluminum composites. *J. Polym. Sci. Part B: Polym. Phys.*, **42**, 722 (2004).
- [13] S.P. Jang, S.U.S. Choi. Role of brownian motion in the enhanced thermal conductivity of nanofluids. *Appl. Phys. Lett.*, **84**, 4316 (2004).
- [14] P.J. Hoogerbrugge, J.M.V.A. Koelman. Simulating microscopic hydrodynamic phenomena with dissipative particle dynamics. *Europhys. Lett.*, **19**, 155 (1992).
- [15] M. Ripoll, M.H. Ernst, P. Espanol. Large scale and mesoscopic hydrodynamic for dissipative particle dynamics. *J. Chem. Phys.*, **115**, 7271 (2001).
- [16] P. Espanol. Dissipative particle dynamics with energy conservation. *Europhys. Lett.*, **40**, 631 (1997).
- [17] J. Bonet-Avalos, A.D. Mackie. Dissipative particle dynamics with energy conservation. *Europhys. Lett.*, **40**, 141 (1997).
- [18] M. Ripoll. Kinetic theory of dissipative particle dynamics models. PhD Thesis, UNED, Madrid, Spain (2002).
- [19] R.D. Groot, P.B. Warren. Dissipative particle dynamics: bridging the gap between atomistic and mesoscopic simulation. *J. Chem. Phys.*, **107**, 4423 (1997).
- [20] P. Nikunen, M. Karttunen, I. Vattulainen. How would you integrate the equations of motion in dissipative particle dynamics simulations. *Comput. Phys. Comm.*, **407** (2003).
- [21] C. Marsh, G. Backx, M.H. Ernst. Static and dynamic properties of dissipative particle dynamics. *Phys. Rev. E*, **56**, 1676 (1997).
- [22] M. Ripoll, M.H. Ernst. Model system for classical fluids out of equilibrium. *Phys. Rev. E*, **71**, 041104 (2004).
- [23] N.S. Martys. Study of a dissipative particle dynamics based approach for modeling suspensions. *J. Rheol.*, **49**, 401 (2005).
- [24] M. Ripoll, P. Español, M.H. Ernst. Dissipative particle dynamics with energy conservation: heat conduction. *Int. J. Mod. Phys. C*, **9**, 1329 (1998).
- [25] S.M. Willemsen, H.C.J. Hoefsloot, D.C. Visser, P.J. Hamersma, P.D. Iedema. Modelling phase change with dissipative particle dynamics using a consistent boundary condition. *J. Comput. Phys.*, **162**, 385 (2000).
- [26] S.M. Willemsen, H.C.J. Hoefsloot, P.D. Iedema. Mesoscopic simulation of polymers in fluid dynamics problems. *J. Stat. Phys.*, **107**, 53 (2002).
- [27] A.F. Jakobsen, O.G. Mouritsen, G. Besold. Artifacts in dynamical simulations of coarse-grained model lipid bilayers. *J. Chem. Phys.*, **122**, 204901 May (2005).
- [28] W. Humphrey, A. Dalke, K. Schulten. VMD—visual molecular dynamics. *J. Mol. Graph.*, **14**, 33 (1996).